

Impact of Impurities on the Thermal Conductivity of Semiconductor Nanostructures: First-Principles Theory

T. M. Gibbons and S. K. Estreicher*

Physics Department, Texas Tech University, Lubbock, Texas 79409-1051, USA

(Received 9 April 2009; published 25 June 2009)

The thermal conductivity $\kappa(T)$ of Si nanostructures containing impurities is calculated from first-principles using nonequilibrium molecular dynamics simulations in thermally “prepared” periodic supercells. For a given concentration of impurities, κ exhibits strongly nonlinear variations with the mass of the impurity. There is a narrow range of conditions for which κ is substantially reduced relative to that of the pure material. This suggests that the κ of nanowire could be controlled with impurities and that nanoregions with a desired κ could be implanted on chips.

DOI: 10.1103/PhysRevLett.102.255502

PACS numbers: 61.72.S-, 63.20.dk, 65.80.+n

The mechanical, electrical, optical, and magnetic properties of semiconductors are controlled by the type and concentration of impurities they contain. For example, the electrical conductivity of Si can be changed by over 8 orders of magnitude with B doping [1,2]. No systematic study of the impact of impurities on the thermal conductivity $\kappa(T)$ of semiconductors is available.

Measurements in *c*-C [3], Si [4] and Ge [5] show that κ increases by about an order of magnitude by isotopic purification. In other words, the inclusion of isotopes (impurities) into pure crystals substantially *decreases* κ . For example, 1.1 at.% of ^{13}C “impurities” in otherwise pure ^{12}C decreases κ by about a factor 10. Is this the maximum that can be achieved? Is the mass of precisely 13 in precisely 1.1 at.% concentration the combination that achieves the maximum possible reduction in κ ? Could different impurity masses, types, and/or concentrations have a greater impact?

Puzzling thermal conductivity data have been reported in alloys. Figure 2 in Ref. [6] shows the measured $\kappa(300\text{ K})$ of $\text{In}_x\text{Ga}_{1-x}\text{N}$, $\text{Al}_x\text{Ga}_{1-x}\text{N}$, and $\text{In}_x\text{Al}_{1-x}\text{N}$ vs x . In $\text{In}_x\text{Ga}_{1-x}\text{N}$ and $\text{Al}_x\text{Ga}_{1-x}\text{N}$, κ decreases by about 1 order of magnitude as x varies from 0.2 to 0.4. But in $\text{In}_x\text{Al}_{1-x}\text{N}$, it increases under the same conditions. If the minority element act as an impurity, then increasing x should increase impurity scattering, and then κ should always decrease with x . But it does not.

Recent calculations [7,8] of thermal conductivities involve *equilibrium* molecular dynamics (MD) simulations. They are based on the Green-Kubo formulation of the fluctuation-dissipation theorem and are normally applied to isotropic systems. The key step is the evaluation of transport coefficients $L_{\alpha\beta} = L_{\beta\alpha}$, defined [8] in terms of correlation functions of the microscopic fluxes of charge (q) and heat (h). If α, β stand for q or h , $L_{\alpha\beta} = \frac{1}{3\Omega} \times \int_0^\infty \langle J_\alpha(t) J_\beta(0) \rangle dt$, where Ω is the volume of the system, $\langle \rangle$ is the average in thermal equilibrium, and $\vec{J}_q = \sum_i Z_i e \vec{v}_i$ and $\vec{J}_h = \frac{d}{dt} \sum_i E_i \vec{r}_i$, where $Z_i e$, \vec{v}_i , E_i , and \vec{r}_i are the nuclear charge, velocity, energy, and position of atom i ,

respectively. Once the three $L_{\alpha\beta}$ coefficients are known, one obtains the electrical conductivity, thermopower and thermal conductivity. The latter is $\kappa = (L_{qq}L_{hh} - L_{qh}^2)/L_{qq}k_B T^2$.

The correlation functions $L_{\alpha\beta}$ converge with difficulty and require simulations lasting hundreds of ps, with time steps of the order of the fs. Thus, empirical potentials have always been used. A first-principles approach is needed when dealing with impurities [9].

The Green-Kubo approach has been used to calculate κ in Si [10] and its frequency-dependence [11], in Si/Ge superlattices [12], and in Ge [13]. Semiempirical nonequilibrium MD (NEMD) have also been used to calculate κ in C nanotubes [14], in Si nanowires [15], and in solid argon [16]. Because of the large temperature fluctuations, large temperature gradients ΔT are needed: 50 and 1000 K in [14]; 66 and 246 K in [16].

We propose here a NEMD approach in “prepared” supercells to calculate $\kappa(T)$ from first principles in periodic supercells containing impurities. The calculations are inspired by experiment: One end of a sample ($x = 0$) is heated with an energy pulse, the heat propagates through the material, and the temperature is recorded at the opposite end ($x = L$) as a function of time. The S -shaped plot of $T(x, t)$ is fit to an equation which contains the thermal diffusivity α , from which the thermal conductivity κ is obtained [17].

We follow the same idea with first-principles theory [9]. We start with a cell repeated N times in one direction of space, producing a N -cells supercell, to which periodic boundary conditions are applied. Since our cells are aligned along $\langle 100 \rangle$, our κ is $\kappa_{\langle 100 \rangle}$.

The key ingredient in the present calculations is the supercell preparation in thermal equilibrium at $t = 0$. This minimizes the T fluctuations, allows us to use small ΔT 's, and remain close to thermal equilibrium. The first cell is prepared in thermal equilibrium at the “hot” temperature T_h . The other $N - 1$ cells are prepared in thermal equilibrium at the “cold” temperature T_c . The hot cell is

appended to the cold cells, and the system is allowed to evolve toward equilibrium. The final temperature is $T_f = \{T_h + (N - 1)T_c\}/N$. We monitor the temperature $T(x, t)$ in the middle cells (Fig. 1) and fit it to the same function used by experimentalists [17]. Adapted to the present configuration, this is

$$T(x, t) = T_c + (T_f - T_c) \sum_n (-1)^n \exp\{-n^2 \pi^2 \alpha t / x^2\}$$

and then $\kappa = \alpha \rho C$, where ρ is the density of the material and C the specific heat at the appropriate temperature. Our sum runs from $n = 0$ to $n = 10$.

Our calculations include quantum corrections [12] to T and κ . These are important below the Debye temperature. However, the functional form we use to fit $T(x, t)$ assumes Fourier's law. This becomes increasingly incorrect as one moves farther away from equilibrium and uses nanoscale systems. The correct heat transfer equation [14,18] involves two unknown relaxation times (for momentum-conserving and umklapp scattering processes, respectively). We ignore this complication for the following reasons. First, we use small ΔT 's and remain close to equilibrium, where deviations from Fourier law are small. Second, we investigate how much κ changes with impurities for a fixed ΔT . The systematic error associated with the absolute value of κ cancel out. Third, since we are using first-principles theory, we are limited to supercells smaller than the Si nanowires measured to date: there are no data to which we can directly compare our results. However, the results of all our tests are consistent with known data: the increase in κ caused by isotopic purity, the reduction in κ with the cross sectional area of the nanowire or supercell and the higher temperature at which κ is maximum, compared to the bulk.

The electronic structure calculations and *ab initio* MD simulations are done with SIESTA [19,20]. Norm-conserving pseudopotentials in the Kleinman-Bylander form [21] describe the core regions. The valence regions are treated within first-principles local density-functional theory with the exchange-correlation potential of Ceperley-Alder [22] parameterized by Perdew-Zunger [23]. The basis sets for the valence states are linear combinations of numerical atomic orbitals [24]. We use double-

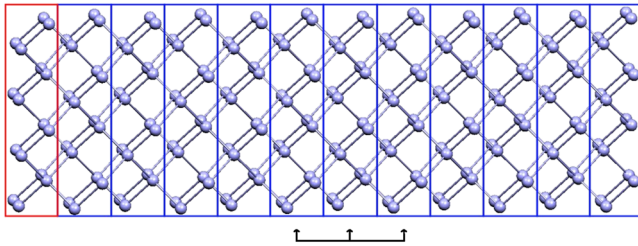


FIG. 1 (color online). The Si_{192} supercell consists of 12 Si_{16} cells prepared in thermal equilibrium, the first one at T_h and the 11 others at T_c . The temperature $T(x, t)$ is monitored in the central cells (arrows).

zeta basis sets (two sets of s and p orbitals for each Si valence state). The charge density is projected on a real-space grid with equivalent cutoffs of 150 Ry to calculate the exchange-correlation and Hartree potentials.

Once the geometry of the system is optimized with maximum force component $F_{\max} < 0.001$ eV/Å, the dynamical matrix is calculated. Its eigenvalues are the normal-mode frequencies ω_s . Its orthonormal eigenvectors $e_{\alpha i}^s$ are used to transform the (harmonic) normal-mode coordinates $q_s = A_s(T) \cos(\omega_s t + \varphi_s)$ into Cartesian nuclear displacements (α numbers the nuclei, $i = x, y, z$):

$$r_{\alpha i} = \frac{1}{\sqrt{m_\alpha}} \sum_s q_s e_{\alpha i}^s.$$

The unknown normal-mode amplitudes A_s are obtained by requiring that, in thermal equilibrium, the *average* kinetic energy of each mode is $k_B T/2$, that is

$$\left\langle \frac{1}{2} \dot{q}_s^2 \right\rangle = \left\langle \frac{1}{2} \omega_s^2 A_s^2 \sin^2(\omega_s t + \varphi_s) \right\rangle = \frac{1}{4} \omega_s^2 \langle A_s^2 \rangle = \frac{1}{2} k_B T.$$

If $A_s = \langle A_s \rangle$, each mode has the energy $k_B T$. Instead, we use a random distribution $\zeta_s = \int_0^{E_s} \{e^{-E/k_B T} / k_B T\} dE$ with $0 < \zeta_s < 1$. Thus, $A_s = \sqrt{-2k_B T \ln(1 - \zeta_s)} / \omega_s$ leads to a distribution of normal-mode energies which averages out to $k_B T$.

Thus, in thermal equilibrium at the temperature T , the Cartesian positions of the nuclei are

$$r_{\alpha i} = \sqrt{\frac{2k_B T}{m_\alpha}} \sum_s \frac{1}{\omega_s} \sqrt{-\ln(1 - \zeta_s)} \cos(\omega_s t + \varphi_s) e_{\alpha i}^s.$$

The initial nuclear positions and velocities in thermal equilibrium are $r_{\alpha i}(t=0)$ and $v_{\alpha i}(t=0) = \dot{r}_{\alpha i}(t=0)$, with random phases $0 \leq \varphi_s < 2\pi$. This supercell preparation for NEMD simulations has been tested in calculations of the T -dependence of vibrational lifetimes [25].

After supercell preparation (1 cell at T_h , 11 cells at T_c), MD simulations are performed without thermostat with a time step $\Delta t = 2.0$ fs. A plot of $T(x, t)$ in the 7th of 12 cells of the Si_{192} supercell after one run and averaged over 10 and 20 runs, respectively, is shown in Fig. 2 with $T_h = 180$ K, $T_c = 120$ K ($T_f = 125$ K). At lower T 's, much smaller ΔT 's can be used. It is equivalent to consider the middle cell and average over 20 to 40 runs with different random φ_s and ζ_s or to average the three middle cells over fewer runs. The increase in κ with isotopic purity of the supercell and a comparison of $\kappa(T)$ between the supercells and Si nanowire data will be discussed elsewhere.

The calculated value, $\kappa(125 \text{ K}) = 2.1 \times 10^{-2}$ W/cm K is larger than, but consistent with, that of Si nanowires of small diameter [26–29]. This discrepancy is anticipated since phonon scattering at the surface reduces the thermal conductivity of nanowires. We use periodic boundary conditions and have no surface. Further, our supercell is isotopically pure ^{28}Si and the nanowires are isotopically mixed. Finally, the cross sectional area of our supercell is smaller

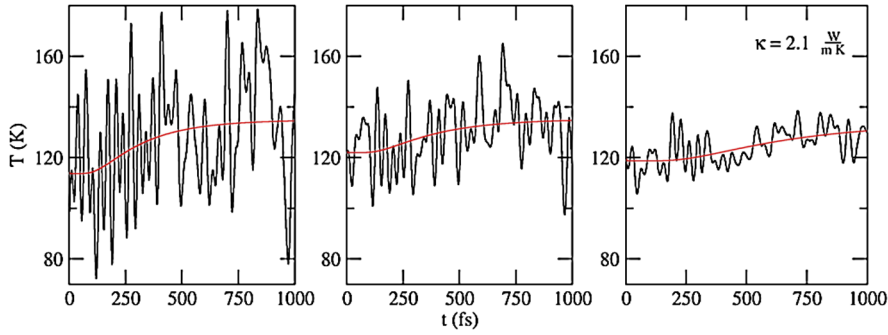


FIG. 2 (color online). Temperature $T(x, t)$ in the 7th cell of $^{28}\text{Si}_{192}$ (Fig. 1) if $T_h = 180$ K and $T_c = 120$ K after 1 run and averaged over 10 and 20 runs, respectively. The fit to $T(x, t)$ (red line) leads to $\kappa(125 \text{ K}) = 2.1 \times 10^{-2} \text{ W/cm K}$.

than that of the smallest nanowire. A 22 nm-diameter nanowire (our 1.5 nm supercell) has $\kappa(125 \text{ K})$ 150 (300) times smaller than the bulk [30]: 6.0 W/cm K. The calculated κ increases with supercell size: Si_{192} , Si_{512} , and Si_{768} have $\kappa(125 \text{ K}) = 2.1 \times 10^{-2}$, 2.6×10^{-2} , and $4.5 \times 10^{-2} \text{ W/cm K}$, respectively.

Impurities perturb the phonon density of states at frequencies that depend on the masses, bond strengths, lattice relaxations, and distortions. The simplest way to vary the impurity-related frequencies is to vary the mass. This requires no additional geometry optimization, and the same force constant matrix can be used to calculate the dynamical matrix and prepare the supercell. We constructed a supercell containing 182 ^{28}Si host atoms and 10 “isotopes” ^MSi , randomly distributed in the supercell. The net impurity concentration is 5 at.%. Then, we calculated $\kappa(M)$ at 125 K. The result is shown in Fig. 3.

The curve shows a sharp minimum at $M = 56$, exactly twice the ^{28}Si mass. We cannot comment about the reasons for this coincidence. We do not know at this time if the factor two remains valid at other temperatures, for concentrations other than 5 at.% and in host crystals other than Si. The shape of $\kappa(M)$ strongly suggests a resonance, as if a 5% concentration of impurities with a specific mass and force constant (in this case, the Si-Si force constant and

oscillator masses 28 and 56, respectively) resulted in a band of localized vibrational modes able to absorb the energy efficiently. $\kappa(125 \text{ K})$ in $^{28}\text{Si}_{182}^{56}\text{Si}_{10}$ is more than 30 times lower than in $^{28}\text{Si}_{192}$.

The figure also shows the result with the 5 at.% of ^MSi replaced by ^{54}Fe , ^{55}Fe , ^{56}Fe , ^{57}Fe . In the case of $^{28}\text{Si}_{182}^{56}\text{Fe}_{10}$, κ is reduced by only a factor of about two. A similar value is obtained with a different random distribution of Fe impurities. The smallest value of κ occurs for ^{55}Fe . Clearly, the mass is not the only factor involved. The bond strength and lattice relaxations must play a role. However, the figure implies that at least one resonance exists, i.e., that it is *a priori* possible to lower κ by a factor of 30 or so.

Impurities heavier than the host atom(s) introducing pseudolocal vibrational modes (pLVMS) [31] which repel the bulk phonons of nearby frequencies. The result is an “island” of localized phonons with long vibrational lifetimes. If such localized modes are resonant with the dominant heat-carrying phonons, they absorb much of the incoming energy and the thermal conductivity drops. In our calculations, this manifests itself by substantially longer MD runs for $M = 56$ before the temperature in the middle cells starts to increase. The pLVMS associated with the heavy Si atoms are shown in Fig. 4.

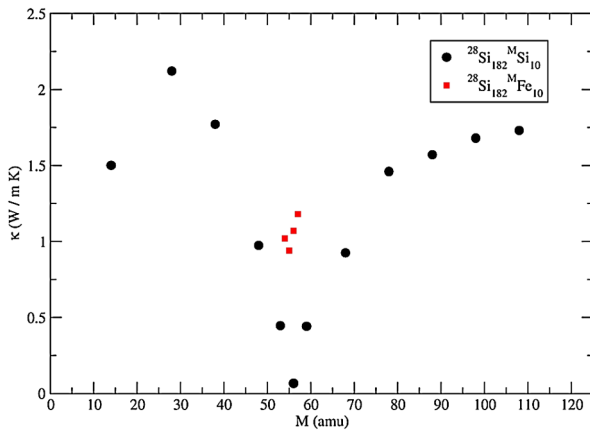


FIG. 3 (color online). Calculated $\kappa(125 \text{ K})$ vs mass M in the $^{28}\text{Si}_{182}^M\text{Si}_{10}$ supercell. The calculation corresponds to a 5 at.% concentration of a substitutional impurity of mass M . The (red) squares show the κ calculated in $^{28}\text{Si}_{182}^M\text{Fe}_{10}$, with $M = 54, 55, 56$, and 57 .

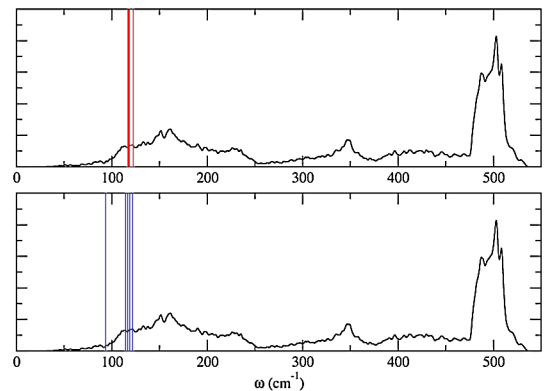


FIG. 4 (color online). Plot of the square of the eigenvectors of the dynamical matrix $|\sum_{i=x,y,z} e_{\alpha i}^s|^2$ with α is a sum over all the ^{56}Si impurities (top figure, red vertical lines) or the ^{56}Fe impurities (bottom figure, blue vertical lines). The background phonon density of states (black) was calculated in the $^{28}\text{Si}_{192}$ supercell with 50 q points.

The key points of this Letter are as follows. (1) We have developed a NEMD scheme to calculate thermal conductivities from first principles in supercells containing arbitrary distributions of impurities, with small T gradients. Even though the method assumes the validity of Fourier's law, the values and calculated behavior of $\kappa(T)$ are consistent with measurements in Si nanowires. However, the central results deal not with the absolute value of κ but on how it *changes* when defects are present in the supercell. (2) For a fixed concentration (we used 5 at.%) of impurities (we used "isotopes" ^MSi), $\kappa(M, T = 125 \text{ K})$ exhibits a sharp minimum at $M = 56$, with $\kappa(M = 56) \leq \kappa(28)/30$. Thus, there is at least one combination of impurity mass and bond strength for which a resonance occurs, the pLVMS associated with the impurities gain energy, the heat flow is dramatically reduced, and κ sharply drops. (3) The existence and position of the minimum of κ depends not just on the impurity mass (the drop is much smaller if we use ^{56}Fe instead of ^{56}Si) but also on the details of the bonding of the impurity to the host crystal. Systematic calculations involving various elements of the Periodic Table are needed in order to uncover which isotope of which "magic" impurity has the maximum impact. The present results show that such effort might be rewarding. (4) The changes in thermal conductivity are unremarkable outside the "resonance" area. (5) It should be possible to control the thermal conductivity of Si nanowire by doping (or of nanochannels on a chip by implanting) carefully selected impurities to achieve a desired thermal conductivity. Implanting a "thermal circuit" on a chip might allow control over thermal gradients. Using impurities to lower the κ of covalent materials is of particular relevance to the thermoelectric figure of merit [32] $ZT = S^2T\sigma/\kappa$ (where S is the Seebeck coefficient and σ the electrical conductivity). A reduction in κ is accompanied by an increase in ZT . In the case of semiconductors, σ is controlled by impurities. The present work shows that κ could be controlled by impurities as well.

This work is supported in part by the Grant No. D-1126 from the R. A. Welch Foundation. Many thanks to Texas Tech's High Performance Computer Center for generous amounts of CPU time.

*stefan.estreicher@ttu.edu

- [1] H. J. Queisser and E. E. Haller, *Science* **281**, 945 (1998).
- [2] H. Temkin and S. K. Estreicher, in *Encyclopedia of Chemical Physics and Physical Chemistry*, edited by J. H. Moore and N. D. Spencer (IOP, Bristol, 2002), Vol. III, p. 2567.
- [3] L. Wei, P. K. Kuo, R. L. Thomas, T. R. Anthony, and W. F. Banholzer, *Phys. Rev. Lett.* **70**, 3764 (1993).
- [4] T. Ruf, R. W. Henn, M. Asen-Palmer, E. Gmelin, M. Cardona, H.-J. Pohl, G. G. Devyatych, and P. G. Sennikov, *Solid State Commun.* **115**, 243 (2000).
- [5] M. Asen-Palmer, K. Bartowski, E. Gmelin, M. Cardona, A. P. Zhernov, A. V. Inyushkin, A. Taldenkov, V. I. Oshogin, K. M. Itoh, and E. E. Haller, *Phys. Rev. B* **56**, 9431 (1997).
- [6] B. N. Pantha, R. Dahal, J. Li, J. Y. Lin, and H. X. Jiang, *Appl. Phys. Lett.* **92**, 042112 (2008).
- [7] M. P. Allen and D. J. Tildesley, *Computer Simulations of Liquids* (Oxford, Clarendon, 2000).
- [8] M. J. Gillan, *Phys. Scr. T* **139**, 362 (1991).
- [9] *Theory of Defects in Semiconductors*, edited by D. A. Drabold and S. K. Estreicher (Springer, Berlin, 2007).
- [10] S. G. Volz and G. Chen, *Phys. Rev. B* **61**, 2651 (2000).
- [11] S. G. Volz, *Phys. Rev. Lett.* **87**, 074301 (2001).
- [12] S. G. Volz, J. B. Saulnier, G. Chen, and P. Beauchamp, *Microelectron. J.* **31**, 815 (2000); S. G. Volz and G. Chen, *Phys. Rev. B* **61**, 2651 (2000).
- [13] H. Ishii, A. Murakawa, and K. Kakimoto, *J. Appl. Phys.* **95**, 6200 (2004).
- [14] J. Shiomi and S. Maruyama, *Phys. Rev. B* **73**, 205420 (2006).
- [15] S. Wang, X. Liang, X. Xu, and T. Ohara, *J. Appl. Phys.* **105**, 014316 (2009).
- [16] S. Volz, J. B. Saulnier, M. Lallemand, B. Perrin, P. Depondt, and M. Mareschal, *Phys. Rev. B* **54**, 340 (1996).
- [17] W. J. Parker, R. J. Jenkins, C. P. Butler, and G. L. Abbot, *J. Appl. Phys.* **32**, 1679 (1961).
- [18] D. D. Joseph and L. Preziosi, *Rev. Mod. Phys.* **61**, 41 (1989); **62**, 375 (1990).
- [19] D. Sánchez-Portal, P. Ordejón, E. Artacho, and J. M. Soler, *Int. J. Quantum Chem.* **65**, 453 (1997).
- [20] E. Artacho, D. Sánchez-Portal, P. Ordejón, A. García, and J. M. Soler, *Phys. Status Solidi (b)* **215**, 809 (1999).
- [21] L. Kleiman and D. M. Bylander, *Phys. Rev. Lett.* **48**, 1425 (1982).
- [22] D. M. Ceperley and B. J. Adler, *Phys. Rev. Lett.* **45**, 566 (1980).
- [23] S. Perdew and A. Zunger, *Phys. Rev. B* **23**, 5048 (1981).
- [24] O. F. Sankey and D. J. Niklevski, *Phys. Rev. B* **40**, 3979 (1989); O. F. Sankey, D. J. Niklevski, D. A. Drabold, and J. D. Dow, *Phys. Rev. B* **41**, 12750 (1990).
- [25] D. West and S. K. Estreicher, *Phys. Rev. Lett.* **96**, 115504 (2006); *Phys. Rev. B* **75**, 075206 (2007).
- [26] D. Li, Y. Wu, P. Kim, L. Shi, P. Yang, and A. Majumdar, *Appl. Phys. Lett.* **83**, 2934 (2003).
- [27] A. I. Hochbaum, R. Chen, R. D. Delgado, W. Liang, E. C. Garnett, M. Najarian, A. Majumdar, and P. Yang, *Nature (London)* **451**, 163 (2008).
- [28] R. Chen, A. I. Hochbaum, P. Murphy, J. Moore, P. Yang, and A. Majumdar, *Phys. Rev. Lett.* **101**, 105501 (2008).
- [29] A. I. Boukai, Y. Bunimovich, J. Tahir-Kheli, J.-K. Yu, W. A. Goddard III, and J. R. Heath, *Nature (London)* **451**, 168 (2008).
- [30] C. J. Glassbrenner and G. A. Slack, *Phys. Rev.* **134**, A1058 (1964).
- [31] S. K. Estreicher, D. West, J. Goss, S. Knack, and J. Weber, *Phys. Rev. Lett.* **90**, 035504 (2003); S. K. Estreicher, D. West, and M. Sanati, *Phys. Rev. B* **72**, 121201(R) (2005).
- [32] M. Apostol, *J. Appl. Phys.* **104**, 053704 (2008).